Am J Transl Res 2023;15(3):1744-1755
www.ajtr.org /ISSN:1943-8141/AJTR0146688

Original Article

Depletion of the m^{6}A demethylases FTO and ALKBH5 impairs growth and metastatic capacity through EMT phenotype change in clear cell renal cell carcinoma

Wei Hu[1,2], Niklas Klümper[1], Doris Schmidt[1], Manuel Ritter[1], Jörg Ellinger[1], Stefan Hauser[1]

[1]Department of Urology, University Hospital Bonn, Bonn, Germany; [2]Department of Urology, Renmin Hospital, Wuhan University, Wuhan, Hubei, China

Received September 25, 2022; Accepted February 22, 2023; Epub March 15, 2023; Published March 30, 2023

Abstract: Background: N^6-methyladenosine (m^{6}A) is one of the most common RNA modifications in eukaryotes and has effects on RNA structure and stability. Recent studies have shown that m^{6}A methylation is involved in human carcinogenesis. In the present study, we investigated the effects of m^{6}A demethylases FTO and ALKBH5 on renal cell carcinoma (RCC) cell lines. Methods: The epithelial-mesenchymal in vitro knockdowns of FTO and ALKBH5 induced by antisense oligonucleotides (LNA-GapmeR system) were established in RCC cell lines. Their effects on migration and proliferation were investigated subsequently. The influence of FTO and ALKBH5 knockdown on key epithelial-mesenchymal transition (EMT) genes was analyzed. Results: Inactivation of FTO and ALKBH5 resulted in decreased proliferation and motility in all cell lines examined (ACHN, Caki-1, 769-P). Vimentin (VIM) was downregulated after the knockdown of FTO and ALKBH5, indicating an EMT switch. Conclusions: Knockdown of the m^{6}A erasers FTO and ALKBH5 inhibits the malignant potential in the cell cultures studied by means of an EMT switch.

Keywords: m^{6}A-erasers, clear cell renal cell carcinoma (ccRCC), epithelial-mesenchymal transition (EMT), FTO, ALKBH5

Introduction

Renal cell carcinoma (RCC) accounts for approximately 3% of all adult cancers and 2% of cancer-related deaths [1, 2]. The prognosis of patients with locally advanced or metastatic RCC is poor. The 5-year survival rate of patients with metastatic RCC is approximately 5% [1, 2]. Modern pharmacotherapy of RCC with tyrosine kinase inhibitors, anti-VEGF antibodies, or checkpoint immunotherapy has only moderately improved patient survival. Complete remission rates of 17% and median overall survival of 40 months are described [3, 4].

RNA methylation was first described in the 1970s. m^{6}A methylation is a dynamic, reversible modification involved in many physiologic processes of eukaryotic cells, such as mRNA localization, translational inhibition or activation, and miRNA processing [5]. M^{6}A methylation affects several important biologic processes, such as tissue development, sex selection, and DNA damage response [6-8]. M^{6}A methylation involves the binding, recognition, and removal of methyl groups from RNA molecules that act as binding proteins, reading proteins, and deletion proteins, respectively [6-8]. If this process is disrupted, abnormal gene expression can occur, leading to a variety of cancers such as leukemia, lung cancer, pancreatic cancer, glioblastoma, and breast cancer [9]. M^{6}A methylation is regulated by enzymes that insert and remove these methylations and are referred to as methylation "writers" and "erasers", respectively. The corresponding localization and activity of these enzymes on chromatin are regulated by chromatin "readers", protein modules that recognize histone and DNA modifications [10, 11]. To date, only two erasers, fat mass and obesity-associated protein (FTO) and AlKBH5 (AlkB family homolog 5), have been discovered [12, 13]. FTO regulates adipogenesis and energy homeostasis [12]. ALKBH5 affects RNA nuclear export and metabolism as well as gene expression [13]. FTO and ALKBH5 are

involved in the carcinogenesis of various tumors [14-16]. Little is known about the role of FTO and ALKBH5 in the genesis of renal cell carcinoma. Strick et al [17] demonstrated that ALKBH5 and FTO are prognostic biomarkers in ccRCC patients, but the functional role of these genes has not been investigated. Epithelial-mesenchymal transition (EMT) is a biologic process in which polarized epithelial cells lose their adhesive properties and adopt a mesenchymal cell phenotype [18]. This process is involved not only in normal embryonic development and tissue repair but is also closely related to the invasion and migration ability of carcinomas. In malignant tumors, EMT is a key process for migration, invasion, metastasis, angiogenesis, and tumorigenicity [18]. It is important to elucidate the regulatory mechanisms of EMT. By understanding these processes, drug therapies can be derived. This could be done by inhibiting tumor cell migration [18].

This study aims to investigate the effects of the knockdown of FTO and ALKBH5 in renal cancer cell lines and to explore the associated mechanisms during EMT and cell proliferation.

Materials and methods

Database analysis and RNAseq expression data

The expression values of FTO and ALKBH5 were obtained from The Cancer Genome Atlas (TCGA; https://cancergenome.nih.gov) and the cBioPortal for Cancer Genomics (https://www.cbioportal.org/) [19, 20]. The log2-transformed RNAseq V2 expression data of ALKBH5 and FTO were compared in the available tumor entities via the cBioportal for Cancer Genomics. Data were processed and normalized using the RSEM method [19, 20].

Cell culture and transfection

The renal carcinoma cell lines ACHN and 769P were purchased from the American Type Culture Collection (Manassas, VA, USA); Caki-1 was purchased from the Deutsche Sammlung von Mikroorganismen und Zellkulturen (Braunschweig, Germany). The cells were cultivated with RPMI Medium 1640 including 5% L-glutamine, 1% penicillin, and 10% fetal bovine serum (all: Gibco, Gaithersburg, MD, USA) at 37°C and 5% CO_2. Cells were seeded in 6-well plates (2×10^5 cells/well). After 24 hours, the cells were transfected with antisense LNA GapmeRs against ALKBH5 or FTO; GapmeRs were designed and synthesized by Qiagen (Hilden, Germany); see Table S1. GapmeRs were labeled with 5'-FAM. Successful transfection was confirmed by fluorescence microscopy after transfection. Transfection was carried out with 10 µl GapmeR, 10 µl FuGENE HD transfection reagent (Promega Mannheim, Germany), and 1980 µl cell culture media. The experiments included an untreated, a negative control GapmeR and a GapmeR against GAPDH. All experiments were carried out in triplicate.

Quantitative real-time polymerase chain reaction (qRT-PCR)

The Total RNA Purification Mini Spin Kit (Genaxxon, Ulm, Germany) was used to isolate total RNA according to the manufacturer's recommendation. Reverse transcription was performed with 1 µg of total RNA using the PrimeScript RT Reagent Kit with gDNA Eraser (Takara Bio, Tokyo, Japan). The expression levels of FTO and ALKBH5 were determined using a QuantStudio5 (Applied Biosystems, Waltham, MA, USA) real-time PCR cycler. cDNAs were amplified using SYBR Green Real-time PCR Master Mix (Takara Bio) and 0.4 µl (10 pmol/µl) of each primer pair. Amplification was performed according to the following protocol: Hot start at 95°C for 30 s, followed by 35 cycles (denaturation at 95°C for 5 s, extension at 60°C for 30 s, preheating at 79°C for 30 s), and concluded with melting curve analysis. All experiments were performed in triplicate on a 384-well plate. Relative expression values were calculated using QuantStudio Design & Analysis software V1.5.1 (Thermo Fisher Scientific, Carlsbad, CA, USA), and expression values were normalized to ACTB expression. Primer sequences are listed in Table S2.

Western blotting

Cell lysates (20 µL) were resolved by SDS-PAGE gel. The separated protein was transferred to the Nitrocellulose membranes (Thermo Fisher Scientific) and subjected to immunoblotting overnight at 4°C (see Table S3 for antibodies). Afterward, incubation with corresponding secondary antibodies (see Table S3) was performed at room temperature for 1 h. After washing with Tris-buffered saline containing

0.1% Tween 20, the blot was developed with WesternBright-ECL-Spray (Advansta, Menlo Park, CA, USA) and images were archived on a Fujifilm LAS-3000 (Fujifilm, Tokyo, Japan) digital photography system.

Cell viability assay

The EZ4U assay (Biomedica, Aschaffenburg, Germany) was used to determine cell viability according to the manufacturer's recommendations. Absorbance was measured at 450 nm with 620 nm as reference using a photometer (Spectra III; Tecan, Crailsheim, Germany) after 3 hours of incubation at 37°C. The cell growth rate was calculated according to the following formula: Cell growth rate (%) = absorbance of the GapmeR group/absorbance of the negative control group × 100%. The cell growth rate of the negative control group was set to 1 (100%). Each cell group included four samples and each experiment was repeated three times. The significance of the treatment was calculated by a t-test using the mean and standard deviation of the growth rate.

Cell migration assay

We used 24-well plates with Falcon Cell Culture Inserts (Thermo Fisher Scientific) for cell migration experiments. Approximately 5×10^4 transfected cells were added to the top of the insert and 300 µl of RPMI Medium 1640 (2% FBS) was added to the specimen. 700 µl of RPMI medium 1640 (20% FBS) was added to the bottom wells to stimulate migration. The cells were incubated at 37°C and 5% CO_2 for 24 hours.

After fixing the cells with 4% paraformaldehyde in phosphate buffer (AppliChem, St. Louis, MO, USA), the nuclei were stained with hematoxylin.

The cells that had not migrated were wiped on the inside of the insert. The migrated cells on the outside of the membrane were mounted on a slide. Photographs of each membrane were taken with a microscope (Olympus DP70, Tokyo, Japan) to evaluate migration. The migrated cells were quantified using QuPath [21]. The cell migration rate was calculated using the following formula: Migration rate (%) = cell number of the gapmeR group/cell number of the negative control group × 100%. The migration rate of the negative control group was set to 1 (100%). Each cell line was run at least 3 times.

Statistical analysis

All measured data were expressed by mean ± standard deviation (mean ± SD). An independent-samples t-test was used to evaluate the significance of the different groups. All data were analyzed using GraphadPrism8.0 software (GraphPad Software, San Diego, CA, USA). Counted data were expressed as % and analyzed by chi-square test. Differences with $P < 0.05$ were considered significant.

Results

First, we analyzed the FTO and ALKBH5 expression profiles in different cancer entities using the Cancer Genome Atlas Research Network (TCGA) datasets with the cBioportal software [19, 20] (**Figure 1**). Of note, both FTO and ALKBH5 expressions were highly expressed in ccRCC. This indicates the functional importance of m^6A demethylases in this particular tumor type.

To better understand the functional role of both highly expressed m^6A demethylases, we performed knockdown experiments to analyze the functional influences of the deletion of FTO and ALKBH5 on parameters of malignancy. After 48 hours of incubation, efficient transfection of fluorescently labeled GapmeRs was evident in the ccRCC cell lines examined. High knockdown efficiency of FTO and ALKBH5 was induced in all cell lines with significantly decreased expression of both genes at both the mRNA and protein levels (see **Figure 2**). Cell proliferation and migration (see **Figures 3** and **4**) were significantly decreased after the knockdown of FTO and ALKBH5 in all cell lines examined. In our opinion, the impaired migratory ability of the cells due to the knockdown of FTO and ALKBH5 was due to the resulting disruption of the EMT signaling pathway.

The GapmeRs of FTO-2 and ALKBH5-2 resulted in the best and most stable reduction of migration and proliferation of the 769-p cell line. Therefore, the GapmeRs (FTO-2 & ALKBH5-2) were selected first to test the RQ-mean of mRNA changes of EMT and proliferation genes of the 769-p cell line. Silencing of FTO or ALKBH5 expression resulted in changes in EMT and proliferation process, for EMT genes (VIM, CDH2, SNAI2) and proliferation genes (PCNA, CDKN1B, P53). Both were significantly downregulated after knockdown of ALKBH5 or FTO in

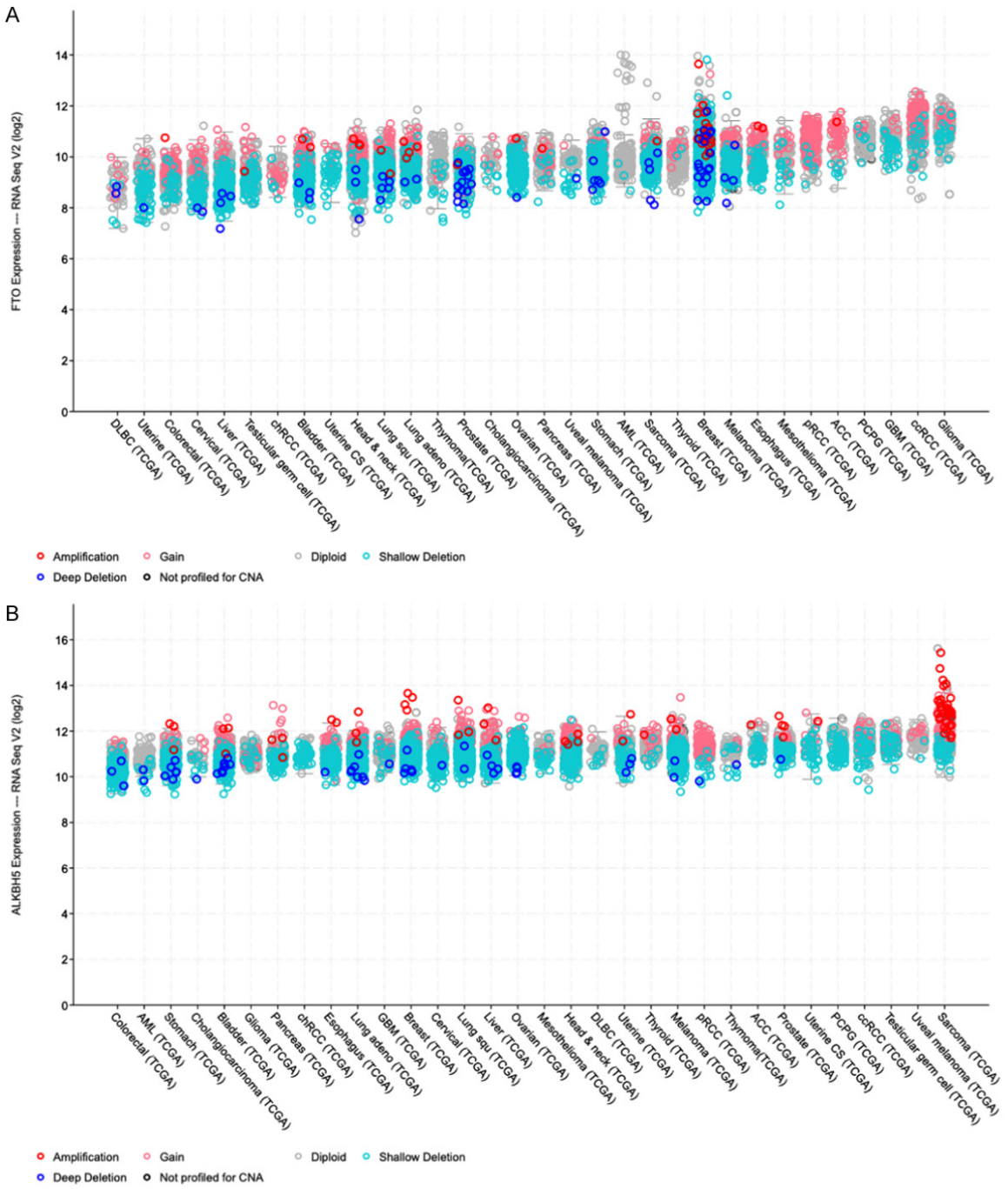

Figure 1. RNAseq expression data of cBioPortal database. A: Available RNA sequencing expression data from 32 cancer entities were studied, and high mRNA expression of FTO in ccRCC, in a pan-cancer analysis of the TCGA (The Cancer Genome Atlas) dataset via cBioportal (cBioPortal for Cancer Genomics, https://www.cbioportal.org), FTO showed the second-highest expression at the transcriptional level in ccRCC. B: Available RNA sequencing expression data from 32 cancer entities were studied, and high mRNA expression of ALKBH5 in ccRCC, in a pan-cancer analysis of the TCGA dataset via cBioportal, ALKBH5 showed the 4th highest expression at the transcriptional level in ccRCC.

RT-PCR. Hereafter, we tested the protein level changes of these six genes. Only VIM and PCNA showed significant results. After specific FTO or ALKBH5 knockdown, we examined VIM expression at the transcriptional and translational levels in 769-P cells.

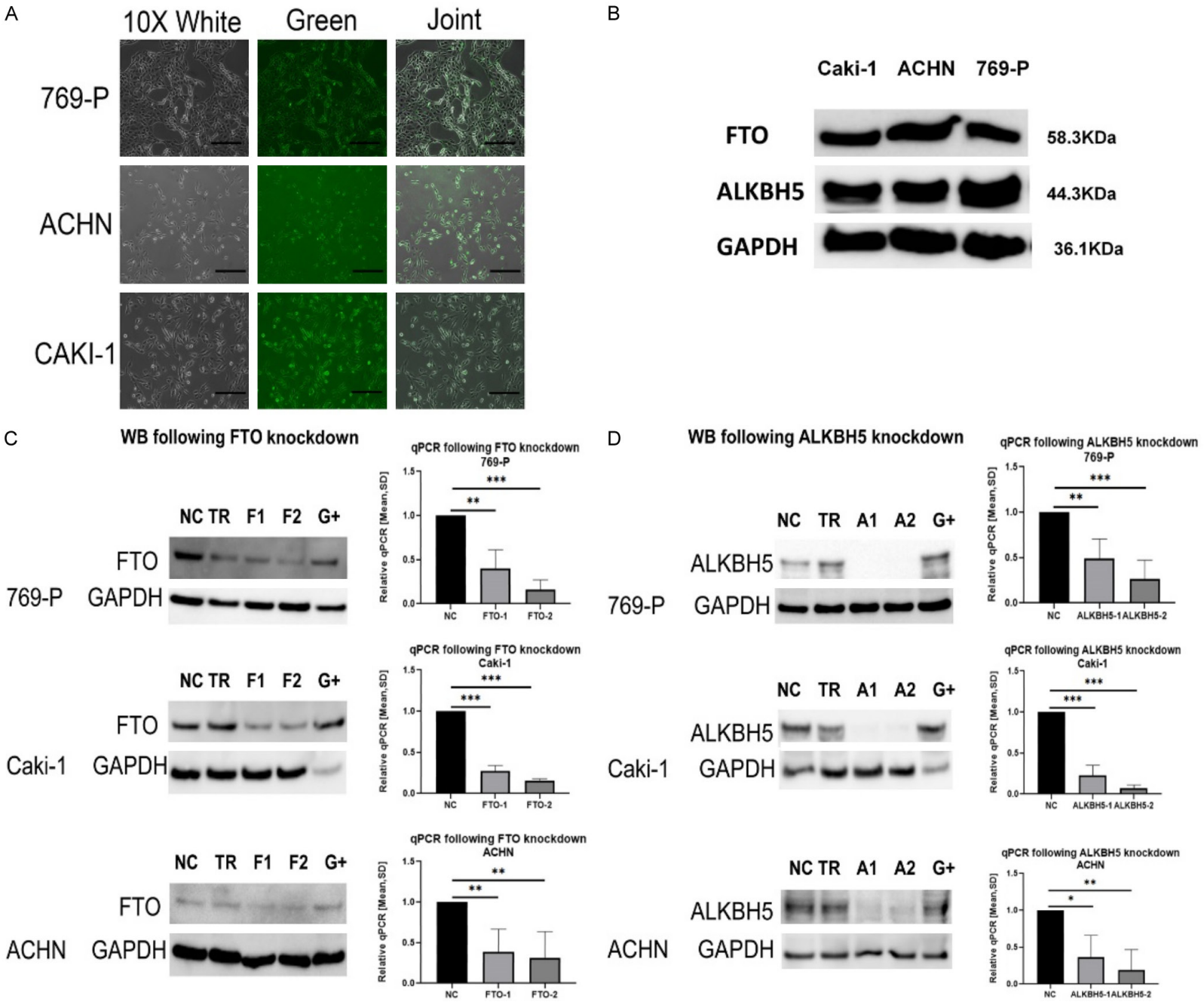
A
10X White
Green
Joint
769-P
ACHN
CAKI-1
B
Caki-1
ACHN
769-P
FTO
58.3KDa
ALKBH5
44.3KDa
GAPDH
36.1KDa
C
WB following FTO knockdown
NC TR F1 F2 G+
FTO
GAPDH
769-P
Caki-1
ACHN
qPCR following FTO knockdown
769-P
Caki-1
ACHN
Relative qPCR [Mean,SD]
NC
FTO-1
FTO-2
D
WB following ALKBH5 knockdown
NC TR A1 A2 G+
ALKBH5
qPCR following ALKBH5 knockdown
ALKBH5-1
ALKBH5-2

Figure 2. Knockdown FTO and ALKBH5 successfully. NT = untreated cells; TR = transfection reagent FuGENE; NC = negative control GapmeR; F1 = FTO-1 GapmeR (Sequence 1); F2 = FTO-2 GapmeR (Sequence 2); A1 = ALKBH5-1 GapmeR (Sequence 1); A2 = ALKBH5-2 GapmeR (Sequence 2); G+ = GAPDH GapmeR (positive control, knock down), all treated cells were collected after transfection GapmeRs for 72 hours; A: All three cell lines, 769-P, Caki-1, and ACHN, show transfection efficiency for all the GapmeRs greater than 90%. The FITC-labeled GapmeRs were transfected with FuGENE HD transfection reagent and photos were taken by a fluorescence microscope. All cells were displayed in the White, green fluorescence GapmeR was observed in the Green and the overlay of both in the Joint picture. B: The protein expression of FTO and ALKBH5 for all three renal cell carcinoma cell lines are detectable and at the correct kD size in western blot analysis. GAPDH was used as a Housekeeper. C: The knockdown effect was determined by real-time PCR and Western blotting. The protein level decreased of FTO compared to Negative Control GapmeR, by at least 50%. The mRNA expression of FTO mRNA relative to the NC group were both significantly downregulated in the renal cancer cell lines (769-P, Caki-1 and ACHN) (ns = no statistically significant; *P < 0.05; **P < 0.01; ***P < 0.001, Student's t-test). D: The knockdown effect was determined by real-time PCR and Western blotting. The protein level decreased of ALKBH5, compared to Negative Control GapmeR, by at least 50%. The mRNA expression of ALKBH5 mRNA relative to the NC group were both significantly downregulated in the renal cancer cell lines (769-P, Caki-1 and ACHN) (ns = no statistically significant; *P < 0.05; **P < 0.01; ***P < 0.001, Student's t-test).

Correlating with the impaired proliferation potential after FTO or ALKBH5 knockdown, the expression of the proliferation marker PCNA was suppressed (see **Figure 5**). In the ccRCC-TCGA cohort, both m^{6}A demethylases were positively correlated with VIM and PCNA expression (see **Figure 6**), in agreement with our experimental results.

Discussion

M^{6}A methylation is the most abundant post-transcriptional modification (> 50%) [22] with the development of high-throughput sequencing technology and advances in epigenetics research [23-26], renewed attention has focused on the function and role of m^{6}A methylation in various biologic processes. M^{6}A methylation differs from other mRNA internal modifications (such as 5-methylcytosine RNA methylation, m^{5}C [27]) because it regulates the post-transcriptional expression level of the gene without altering the base sequence. This is mainly done by affecting the binding of the mRNA to the writing protein. This regulates the splicing, translation, and stabilization of the mRNA. This process is reversible and precisely controlled. This process involves 3 steps: ① Methylation, the enzyme that adds the methyltransferase (writer); ② Demethylation, i.e. the methyl group is removed, the methyl group is stripped from the carbocyclic ring by a demethylase (eraser); ③ Binding: the RNA base sites where the methylation is changed are recognized and bound.

Several studies have shown that aberrant m^{6}A levels are associated with carcinogenesis in human malignancies [14-16]. Methylation "writers" (consisting of METTL3, METTL14, and WTAP) mediate m^{6}A modification of RNA, while two distinct proteins (FTO and ALKBH5) mediate demethylation. So far, it is not known whether the only human m^{6}A eraser proteins FTO and ALKBH5 have distinct or redundant functions [10-12], FTO and ALKBH5 are abnormally expressed in many tumors [14-16]. FTO plays a critical role in carcinogenesis as an m^{6}A eraser. R-2HG targets the FTO/m^{6}A/MYC/CEBPA axis and has antitumor activity in leukemia and brain tumors [9, 14, 28]. ALKBH5 is known to affect mRNA export and RNA metabolism. In the pathogenesis of glioblastoma and breast cancer, ALKBH5 acts as an oncoprotein by affecting the proliferation and self-renewal of cancer stem cells [15, 16, 29]. ALKBH5 expression is abnormally upregulated in glioblastoma cells, and its increased expression is associated with poor disease outcome in patients with glioblastoma multiforme [15]. Suppression of ALKBH5 expression in hypoxic MCF-7 and MDA-MB-231 cells increased the m^{6}A content of the total cellular RNA pool, indicating that ALKBH5 plays an important role in regulating RNA methylation in human breast cancer cells [16, 29]. The function of m^{6}A demethylases in RCC is poorly understood.

We observed that the expression levels of the two M^{6}A demethylases studied were comparatively high in ccRCC, suggesting their possible importance in the pathogenesis of this tumor entity. We knocked down FTO and ALKBH5 in RCC cell lines (769-P, Caki-1, ACHN) using gapmeRs. A decrease in FTO and ALKBH5 gene expression inhibited proliferation and migration

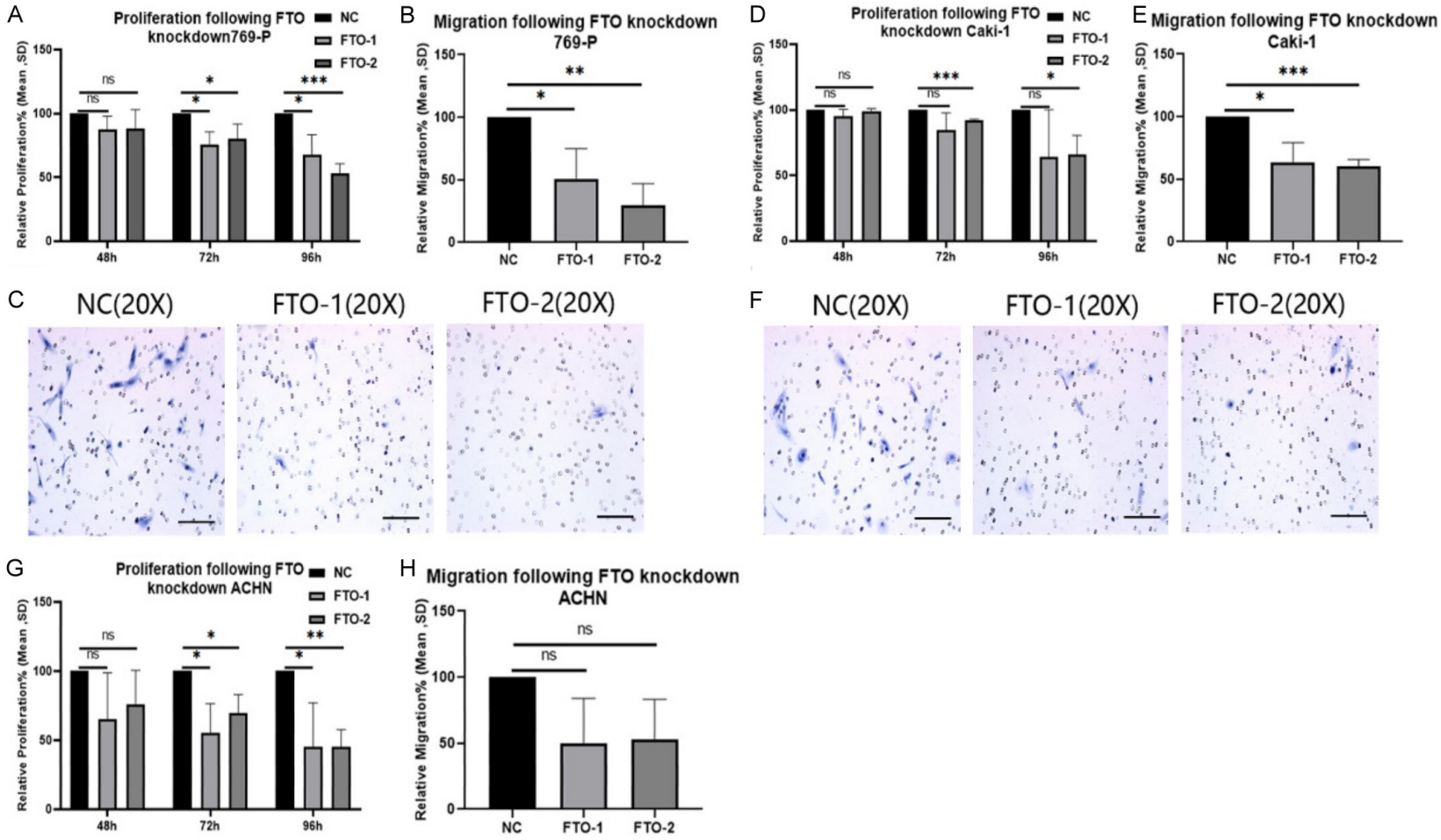

Figure 3. Knockdown of FTO decreased migration and proliferation for all studied cell lines. A: Effects of knocking down FTO on 769-P cell lines respectively growth/proliferation by EZ4U test. (ns = not statistically significant; *P < 0.05; **P < 0.01; ***P < 0.001, Student's t-test). B: Effects of knocking down FTO on 769-P cell lines. Results show the migration capacity by cell count analysis on Boyden chamber membranes. (ns = not statistically significant; *P < 0.05; **P < 0.01; ***P < 0.001, Student's t-test). C: Pictures of cell count analysis on Boyden chamber membranes by 20 × microscopy to demonstrate migration after 24 h. The effect of FTO knocking down on 769-P cell lines. The ACHN showed no statistically significant difference, so we did not show the changes by 20 × microscopy. D: Effects of knocking down FTO on Caki-1 cell lines respectively growth/proliferation by EZ4U test. (ns = not statistically significant; *P < 0.05; **P < 0.01; ***P < 0.001, Student's t-test). E: Effects of knocking down FTO on Caki-1 cell lines respectively migration capacity by cell count analysis on Boyden chamber membranes. (ns = not statistically significant; *P < 0.05; **P < 0.01; ***P < 0.001, Student's t-test). F: Pictures of cell count analysis on Boyden chamber membranes by 20 × microscopy to demonstrate migration after 24 h. The effect of FTO knocking down on Caki-1 cell lines. The ACHN showed no statistical significance, so we do not show the changes of 20 × microscopy. G: Effects of knocking down FTO on ACHN cell lines respectively. Growth/proliferation by EZ4U test. (ns = not statistically significant; *P < 0.05; **P < 0.01; ***P < 0.001, Student's t-test). H: Effects of knocking down FTO on ACHN cell lines respectively migration capacity by cell count analysis on Boyden chamber membranes. (ns = not statistically significant; *P < 0.05; **P < 0.01; ***P < 0.001, Student's t-test).

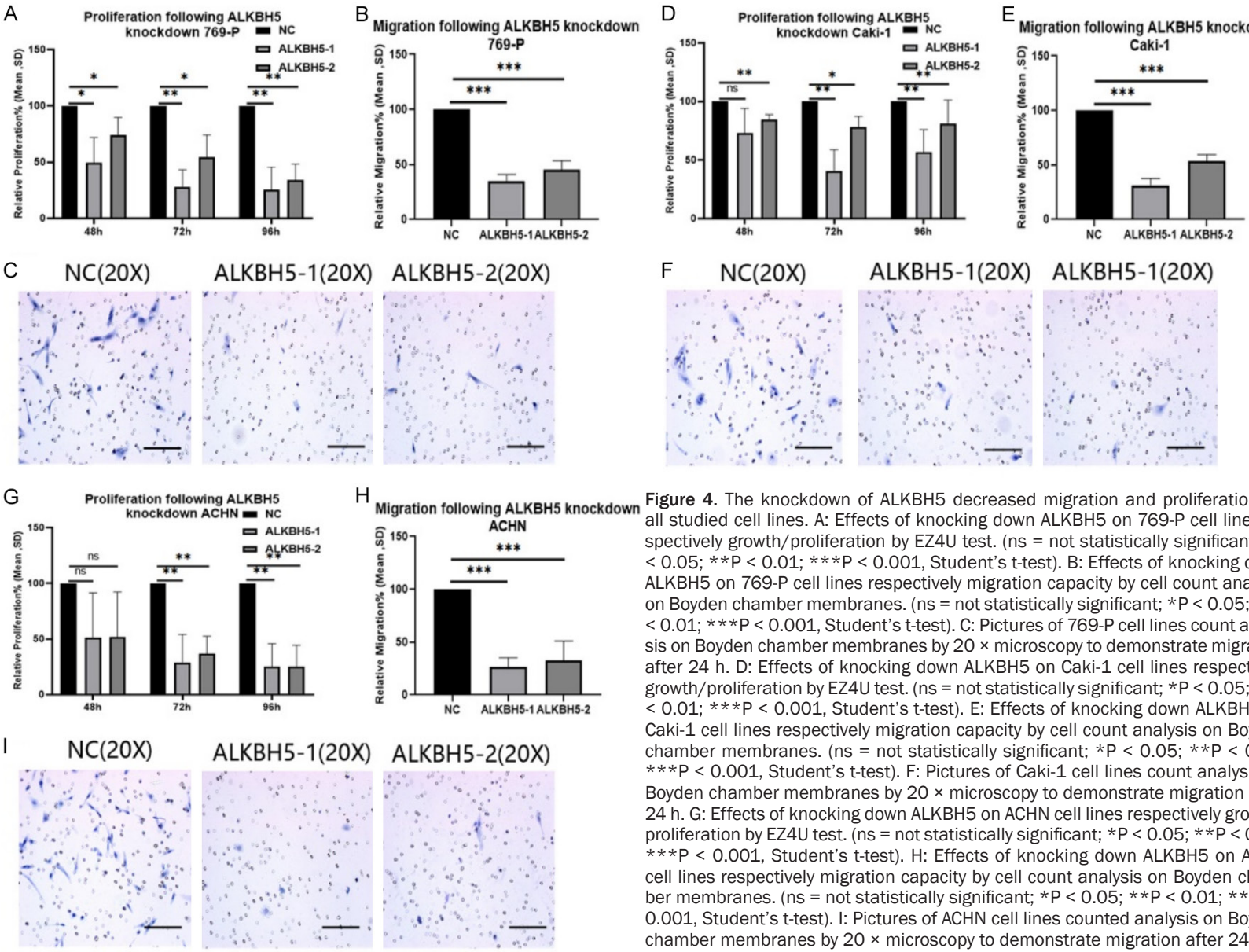

Figure 4. The knockdown of ALKBH5 decreased migration and proliferation for all studied cell lines. A: Effects of knocking down ALKBH5 on 769-P cell lines respectively growth/proliferation by EZ4U test. (ns = not statistically significant; *P < 0.05; **P < 0.01; ***P < 0.001, Student's t-test). B: Effects of knocking down ALKBH5 on 769-P cell lines respectively migration capacity by cell count analysis on Boyden chamber membranes. (ns = not statistically significant; *P < 0.05; **P < 0.01; ***P < 0.001, Student's t-test). C: Pictures of 769-P cell lines count analysis on Boyden chamber membranes by 20 × microscopy to demonstrate migration after 24 h. D: Effects of knocking down ALKBH5 on Caki-1 cell lines respectively growth/proliferation by EZ4U test. (ns = not statistically significant; *P < 0.05; **P < 0.01; ***P < 0.001, Student's t-test). E: Effects of knocking down ALKBH5 on Caki-1 cell lines respectively migration capacity by cell count analysis on Boyden chamber membranes. (ns = not statistically significant; *P < 0.05; **P < 0.01; ***P < 0.001, Student's t-test). F: Pictures of Caki-1 cell lines count analysis on Boyden chamber membranes by 20 × microscopy to demonstrate migration after 24 h. G: Effects of knocking down ALKBH5 on ACHN cell lines respectively growth/proliferation by EZ4U test. (ns = not statistically significant; *P < 0.05; **P < 0.01; ***P < 0.001, Student's t-test). H: Effects of knocking down ALKBH5 on ACHN cell lines respectively migration capacity by cell count analysis on Boyden chamber membranes. (ns = not statistically significant; *P < 0.05; **P < 0.01; ***P < 0.001, Student's t-test). I: Pictures of ACHN cell lines counted analysis on Boyden chamber membranes by 20 × microscopy to demonstrate migration after 24 h.

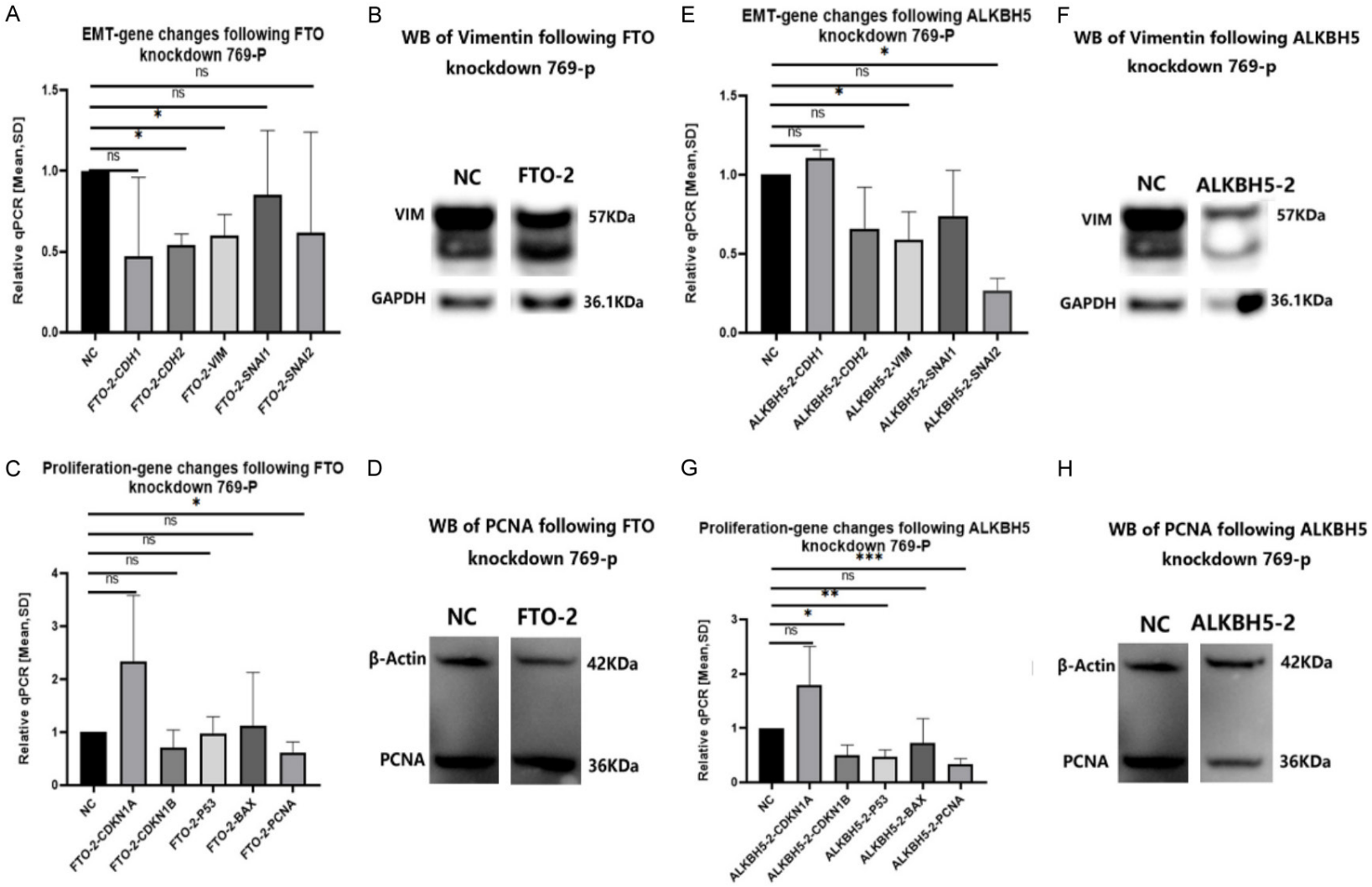

Figure 5. Effects of EMT and proliferation genes changes by knockdown FTO or ALKBH5 on 769-P. Our GapmeRs of FTO-2 and ALKBH5-2 show the best and most stable results on migration and proliferation of the 769-p cell line, so we choose GapmeRs (FTO-2 & ALKBH5-2) to test the RQ-mean of mRNA changes on EMT and Proliferation Genes of 769-p cell line. Silencing FTO and ALKBH5 expression resulted in alterations in the EMT and proliferation process. A: From the RT-PCR results of EMT genes, we found Vimentin (VIM) and N-Cadherin (CDH2) downregulated with statistical significance after FTO knockdown. (ns = not statistically significant; *P < 0.05; **P < 0.01; ***P < 0.001, Student's t-test). B: The protein of VIM was downregulated as well in the western blot experiment. (ns = not statistically significant; *P < 0.05; **P < 0.01; ***P < 0.001, Student's t-test). C: The RT-PCR results of proliferation genes demonstrate a statistically significant downregulation of PCNA after FTO knockdown. (ns = not statistically significant; *P < 0.05; **P < 0.01; ***P < 0.001, Student's t-test). D: There was no significant downregula-

tion of PCNA after FTO knockdown on the protein level of PCNA. (ns = not statistically significant; *P < 0.05; **P < 0.01; ***P < 0.001, Student's t-test). E: VIM and Snail Family Transcriptional Repressor 2 (SNAI2) were significantly downregulated after ALKBH5 knockdown in RT-PCR. (ns = not statistically significant; *P < 0.05; **P < 0.01; ***P < 0.001, Student's t-test). F: We used VIM to correlate this knockdown effect on the protein level. Change of Proliferation Genes for mRNA and proteins after Silencing FTO-2 and ALKBH5-2 in the 769-p cell line. The genes of CDKN1A, CDKN1B, p53, BAX, and PCNA were tested. (ns = not statistically significant; *P < 0.05; **P < 0.01; ***P < 0.001, Student's t-test). G: CDKN1B, p53 and PCNA mRNA were downregulated with statistic significance after ALKBH5 knockdown. (ns = not statistically significant; *P < 0.05; **P < 0.01; ***P < 0.001, Student's t-test). H: The protein of PCNA was also downregulated following ALKBH5 knockdown. (ns = not statistically significant; *P < 0.05; **P < 0.01; ***P < 0.001, Student's t-test).

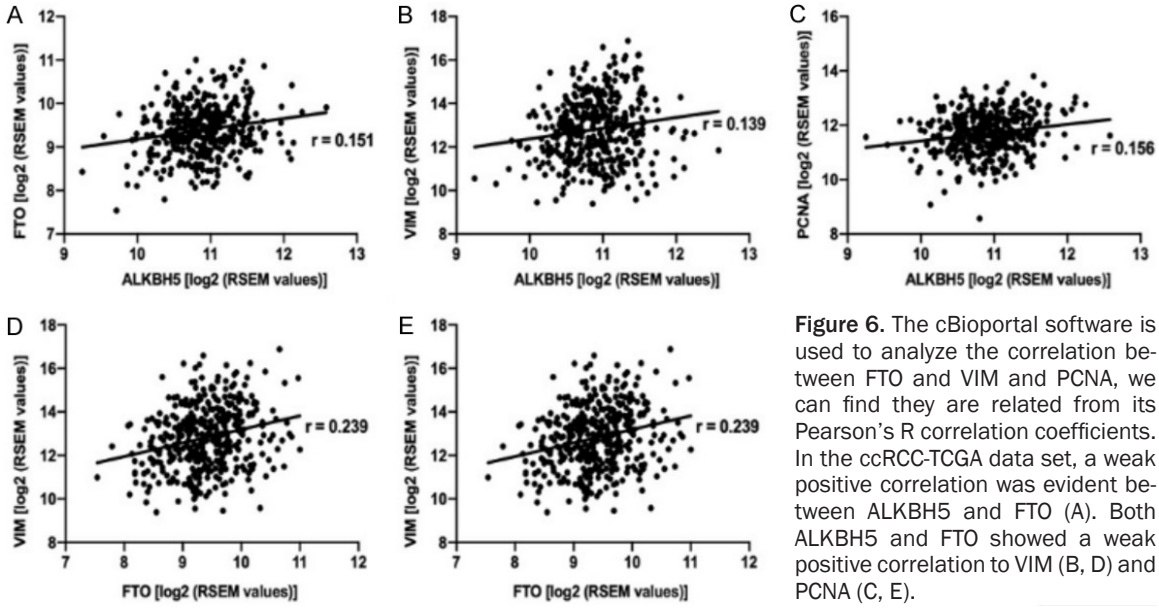

Figure 6. The cBioportal software is used to analyze the correlation between FTO and VIM and PCNA, we can find they are related from its Pearson's R correlation coefficients. In the ccRCC-TCGA data set, a weak positive correlation was evident between ALKBH5 and FTO (A). Both ALKBH5 and FTO showed a weak positive correlation to VIM (B, D) and PCNA (C, E).

in the cell lines studied. Epithelial cells can undergo epithelial-mesenchymal transition (EMT) to transform into highly motile and invasive phenotypes and migrate from the original tissue. EMT is therefore a crucial step in cancer progression [18, 30-33].

Suppression of FTO and ALKBH5 expression resulted in changes in the EMT (indicated by altered VIM mRNA/protein expression) and proliferation (altered PCNA mRNA/protein expression) axes. Accordingly, m^6A demethylases affect ccRCC progression through changes in EMT and proliferation.

In summary, we demonstrated that the m^6A demethylases FTO and ALKBH5 play an oncogenic role by promoting cell migration and proliferation through modulation of the epithelial-mesenchymal transition and cell cycle. The genes involved are VIM and PCNA. The mechanism by which other genes such as CDH2, SNAI2 among EMT genes and CDKN1B, and P53 regulating proliferation are involved in this process is currently unclear and needs further investigation. FTO and ALKBH5 are highly expressed in renal cancer and may represent therapeutic targets for the treatment of renal cancer.

Acknowledgements

WH was supported by grant No. 2019CFB743 from the Hubei Province Natural Science Foundation, China.

The experimental protocol was established, according to the ethical guidelines of the Helsinki Declaration and was approved by the Human Ethics Committee of University Hospital Bonn. Written informed consent was obtained from individual or guardian participants.

Disclosure of conflict of interest

None.

Address correspondence to: Dr. Wei Hu, Department of Urology, Renmin Hospital, Wuhan University, Jiefang Road 238#, Wuhan 430060, Hubei, China. Tel: +86-2788041911-83325; Fax: +86-2788041911-83326; E-mail: shakurase1@163.com; Dr. Stefan Hauser, Universitätsklinikum Bonn, Klinik und Poliklinik für Urologie und Kinderurologie, Bonn, Germany. Tel: +49-228-287-14184; Fax: +49-228-287-14185; E-mail: stefan.hauser@ukbonn.de

References

[1] Amin MB, Greene FL, Edge SB, Compton CC, Gershenwald JE, Brookland RK, Meyer L, Gress DM, Byrd DR and Winchester DP. The eighth edition AJCC cancer staging manual: continuing to build a bridge from a population-based to a more "personalized" approach to cancer staging. CA Cancer J Clin 2017; 67: 93-99.

[2] Jonasch E, Walker CL and Rathmell WK. Clear cell renal cell carcinoma ontogeny and mechanisms of lethality. Nat Rev Nephrol 2021; 17: 245-261.

[3] Choueiri TK and Motzer RJ. Systemic therapy for metastatic renal-cell carcinoma. N Engl J Med 2017; 376: 354-366.

[4] Trott JF, Kim J, Abu Aboud O, Wettersten H, Stewart B, Berryhill G, Uzal F, Hovey RC, Chen CH, Anderson K, Graef A, Sarver AL, Modiano JF and Weiss RH. Inhibiting tryptophan metabolism enhances interferon therapy in kidney cancer. Oncotarget 2016; 7: 66540-66557.

[5] Dubin DT and Taylor RH. The methylation state of poly A-containing messenger RNA from cultured hamster cells. Nucleic Acids Res 1975; 2: 1653-1668.

[6] Jia G, Fu Y and He C. Reversible RNA adenosine methylation in biological regulation. Trends Genet 2013; 29: 108-115.

[7] Liu N and Pan T. N6-methyladenosine-encoded epitranscriptomics. Nat Struct Mol Biol 2016; 23: 98-102.

[8] Wang T, Kong S, Tao M and Ju S. The potential role of RNA N6-methyladenosine in cancer progression. Mol Cancer 2020; 19: 88.

[9] Deng X, Su R, Feng X, Wei M and Chen J. Role of N(6)-methyladenosine modification in cancer. Curr Opin Genet Dev 2018; 48: 1-7.

[10] Torres IO and Fujimori DG. Functional coupling between writers, erasers and readers of histone and DNA methylation. Curr Opin Struct Biol 2015; 35: 68-75.

[11] Yang Y, Hsu PJ, Chen YS and Yang YG. Dynamic transcriptomic m^6A decoration: writers, erasers, readers and functions in RNA metabolism. Cell Res 2018; 28: 616-624.

[12] Zheng G, Dahl JA, Niu Y, Fedorcsak P, Huang CM, Li CJ, Vågbø CB, Shi Y, Wang WL, Song SH, Lu Z, Bosmans RP, Dai Q, Hao YJ, Yang X, Zhao WM, Tong WM, Wang XJ, Bogdan F, Furu K, Fu Y, Jia G, Zhao X, Liu J, Krokan HE, Klungland A, Yang YG and He C. ALKBH5 is a mammalian RNA demethylase that impacts RNA metabolism and mouse fertility. Mol Cell 2013; 49: 18-29.

[13] Jia G, Fu Y, Zhao X, Dai Q, Zheng G, Yang Y, Yi C, Lindahl T, Pan T, Yang YG and He C. N6-methyladenosine in nuclear RNA is a major substrate of the obesity-associated FTO. Nat Chem Biol 2011; 7: 885-887.

[14] Li Z, Weng H, Su R, Weng X, Zuo Z, Li C, Huang H, Nachtergaele S, Dong L, Hu C, Qin X, Tang L, Wang Y, Hong GM, Huang H, Wang X, Chen P, Gurbuxani S, Arnovitz S, Li Y, Li S, Strong J, Neilly MB, Larson RA, Jiang X, Zhang P, Jin J, He C and Chen J. FTO plays an oncogenic role in acute myeloid leukemia as a N(6)-methyladenosine RNA demethylase. Cancer Cell 2017; 31: 127-141.

[15] Zhang S, Zhao BS, Zhou A, Lin K, Zheng S, Lu Z, Chen Y, Sulman EP, Xie K, Bögler O, Majumder S, He C and Huang S. m(6)A demethylase ALKBH5 maintains tumorigenicity of glioblastoma stem-like cells by sustaining FOXM1 expression and cell proliferation program. Cancer Cell 2017; 31: 591-606, e6.

[16] Zhang C, Samanta D, Lu H, Bullen JW, Zhang H, Chen I, He X and Semenza GL. Hypoxia induces the breast cancer stem cell phenotype by HIF-dependent and ALKBH5-mediated m^6A-demethylation of NANOG mRNA. Proc Natl Acad Sci U S A 2016; 113: E2047-2056.

[17] Strick A, von Hagen F, Gundert L, Klümper N, Tolkach Y, Schmidt D, Kristiansen G, Toma M, Ritter M and Ellinger J. The N(6)-methyladenosine (m(6)A) erasers alkylation repair homologue 5 (ALKBH5) and fat mass and obesity-associated protein (FTO) are prognostic biomarkers in patients with clear cell renal carcinoma. BJU Int 2020; 125: 617-624.

[18] Tretbar S, Krausbeck P, Müller A, Friedrich M, Vaxevanis C, Bukur J, Jasinski-Bergner S and Seliger B. TGF-β inducible epithelial-to-mesenchymal transition in renal cell carcinoma. Oncotarget 2019; 10: 1507-1524.

[19] Cerami E, Gao J, Dogrusoz U, Gross BE, Sumer SO, Aksoy BA, Jacobsen A, Byrne CJ, Heuer ML, Larsson E, Antipin Y, Reva B, Goldberg AP, Sander C and Schultz N. The cBio cancer genomics portal: an open platform for exploring multidimensional cancer genomics data. Cancer Discov 2012; 2: 401-404.

[20] Gao J, Aksoy BA, Dogrusoz U, Dresdner G, Gross B, Sumer SO, Sun Y, Jacobsen A, Sinha R, Larsson E, Cerami E, Sander C and Schultz N. Integrative analysis of complex cancer genomics and clinical profiles using the cBioPortal. Sci Signal 2013; 6: pl1.

[21] Bankhead P, Loughrey MB, Fernández JA, Dombrowski Y, McArt DG, Dunne PD, McQuaid S, Gray RT, Murray LJ, Coleman HG, James JA, Salto-Tellez M and Hamilton PW. QuPath: open source software for digital pathology image analysis. Sci Rep 2017; 7: 16878.

[22] Fu Y, Dominissini D, Rechavi G and He C. Gene expression regulation mediated through reversible m^6A RNA methylation. Nat Rev Genet 2014; 15: 293-306.

[23] Boccaletto P, Machnicka MA, Purta E, Piatkowski P, Baginski B, Wirecki TK, de Crécy-Lagard V, Ross R, Limbach PA, Kotter A, Helm M and Bujnicki JM. MODOMICS: a database of RNA modification pathways. 2017 update. Nucleic Acids Res 2018; 46: D303-D307.

[24] Tost J and Gut IG. DNA methylation analysis by pyrosequencing. Nat Protoc 2007; 2: 2265-2275.

[25] Trinh BN, Long TI and Laird PW. DNA methylation analysis by MethyLight technology. Methods 2001; 25: 456-462.

[26] Schwartz S and Motorin Y. Next-generation sequencing technologies for detection of modified nucleotides in RNAs. RNA Biol 2017; 14: 1124-1137.

[27] Motorin Y, Lyko F and Helm M. 5-methylcytosine in RNA: detection, enzymatic formation and biological functions. Nucleic Acids Res 2010; 38: 1415-1430.

[28] Huang Y, Su R, Sheng Y, Dong L, Dong Z, Xu H, Ni T, Zhang ZS, Zhang T, Li C, Han L, Zhu Z, Lian F, Wei J, Deng Q, Wang Y, Wunderlich M, Gao Z, Pan G, Zhong D, Zhou H, Zhang N, Gan J, Jiang H, Mulloy JC, Qian Z, Chen J and Yang CG. Small-molecule targeting of oncogenic FTO demethylase in acute myeloid leukemia. Cancer Cell 2019; 35: 677-691, e10.

[29] Zhang C, Zhi WI, Lu H, Samanta D, Chen I, Gabrielson E and Semenza GL. Hypoxia-inducible factors regulate pluripotency factor expression by ZNF217- and ALKBH5-mediated modulation of RNA methylation in breast cancer cells. Oncotarget 2016; 7: 64527-64542.

[30] Kim T, Veronese A, Pichiorri F, Lee TJ, Jeon YJ, Volinia S, Pineau P, Marchio A, Palatini J, Suh SS, Alder H, Liu CG, Dejean A and Croce CM. p53 regulates epithelial-mesenchymal transition through microRNAs targeting ZEB1 and ZEB2. J Exp Med 2011; 208: 875-883.

[31] Strouhalova K, Přechová M, Gandalovičová A, Brábek J, Gregor M and Rosel D. Vimentin intermediate filaments as potential target for cancer treatment. Cancers (Basel) 2020; 12: 184.

[32] Satelli A and Li S. Vimentin in cancer and its potential as a molecular target for cancer therapy. Cell Mol Life Sci 2011; 68: 3033-3046.

[33] Yin S, Chen FF and Yang GF. Vimentin immunohistochemical expression as a prognostic factor in gastric cancer: a meta-analysis. Pathol Res Pract 2018; 214: 1376-1380.

Table S1. The GapmeR sequences of all the genes

Target	Sequence
FTO-1	CTTTACGCAGCTTGAT
FTO-2	ACCAGTCACTCATTAA
ALKBH5-1	AGCAATTGAGGACATC
ALKBH5-2	GTAAAGTCAAGAGGTT
Neg Ctrl A	AACACGTCTATACGC
GAPDH	AGATTCAGTGTGGTGG

Table S2. The PCR primer sequences of all the genes

Target	Sequence
ACTB-forward	CCAACCGCGAGAAGATGA
ACTB-reverse	CCAGAGGCGTACAGGGATAG
GAPDH-forward	CTCTGCTCCTCCTGTTCGAC
GAPDH-reverse	ACGACCAAATCGGTTGACTC
ALKBH5-forward	CCTGCTCTGAAACCCAAGC
ALKBH5-reverse	TCCTTGTCCATCTCCAGGAT
FTO-forward	GAAAATCTGGTGGACAGGTCA
FTO-reverse	CGAGATGAGAGTCATCCTCACTT
CDKN1A-forward	CGAAGTCAGTTCCTTGTGGAG
CDKN1A-reverse	CATGGGTTCTGACGGACAT
CDKN1B-forward	CCCTAGAGGGCAAGTACGAGT
CDKN1B-reverse	AGTAGAACTCGGGCAAGCTG
BAX-forward	ATGTTTTCTGACGGCAACTTC
BAX-reverse	ATCAGTTCCGGCACCTTG
P53-forward	CTTTCCACGACGGTGACA
P53-reverse	TCCTCCATGGCAGTGACC
CDH1-forward	AAGGGGTCTGTCATGGAAGG
CDH1-reverse	GGTGTTCACATCATCGTCCG
CDH2-forward	CCATCATTGCCATCCTGCTC
CDH2-reverse	GTTTGGCCTGGCGTTCTTTA
SNAI1-forward	GCTGCAGGACTCTAATCCAGA
SNAI1-reverse	ATCTCCGGAGGTGGGATG
SNAI2-forward	TGGTTGCTTCAAGGACACAT
SNAI2-reverse	GTTGCAGTGAGGGCAAGAA
VIM-forward	GAGAGGAAGCCGAAAACACC
VIM-reverse	TTGCGTTCAAGGTCAAGACG
PCNA-forward	TGTCACAGACAAGTAATGTCGATAAA
PCNA-reverse	GAACTGGTTCATTCATCTCTATGG

Table S3. The antibody information of all the genes

Specific Antibody	Dilution	Manufacturer
Anti-FTO	IgG rabbit 1:1250	Atlas Antibodies, Bromma, Sweden
Anti-ALKBH5	IgG rabbit 1:250	Novus Biologicals, Centennial, USA
Anti-VIM	IgG rabbit 1:1000	Cell Signaling Technology, Danvers, USA
Anti-PCNA	IgG mouse 1:200	Santa Cruz Biotechnology, Dallas, USA
Anti-CDH2	IgG mouse 1:200	Santa Cruz Biotechnology, Dallas, USA
Anti-SNAI2	IgG mouse 1:100	Santa Cruz Biotechnology, Dallas, USA
Anti-CDKN1B	IgG mouse 1:200	Santa Cruz Biotechnology, Dallas, USA
Anti-P53	IgG mouse 1:200	Santa Cruz Biotechnology, Dallas, USA
Anti-GAPDH	IgG rabbit 1:1000	Cell Signaling Technology, Danvers, USA
Anti-β-Actin	IgG-mouse 1:5000	Sigma-Aldrich, St. Louis, USA
Secondary Antibody	Dilution	manufacturer
Anti-Rabbit-POD	IgG-rabbit 1:2000	Cell Signaling Technology, Danvers, USA
Anti-mouse-POD	IgG-mouse 1:3000	BIO-RAD Laboratories, Hercules, USA

We use Anti-Rabbit-POD as secondary antibody for IgG-rabbit specific antibody, and Anti-mouse-POD as secondary antibody for IgG-mouse specific antibody.